

Optimization of Electrode Positions of a Wearable ECG Monitoring System for Efficient and Effective Detection of Acute Myocardial Infarction

Y Jiang, C Qian, R Hanna, D Farina, O Doessel

Karlsruhe Institute of Technology (KIT), Karlsruhe, Germany

Abstract

Acute myocardial infarction is one of the leading causes of morbidity and mortality all over the world. Therefore, it is of very high importance to detect myocardial infarction effectively and accurately in its early phase with an efficient method. Electrocardiogram provides a non-invasive and inexpensive way for diagnosis of myocardial infarction through seeking for the ischemic syndromes in ECG, e.g., the elevation or depression of ST-segment. However, the standard 12 lead ECG does not examine the heart from all aspects. On the other hand, the comprehensive body surface potential mapping system is nearly impossible to be wearable. In the present project a wearable ECG monitoring system for detection of acute myocardial infarction is optimized with respect to electrode positions. The optimal electrode configuration suggested in the present study includes 2 pairs of electrodes and a high sensitivity of 98% is achieved in the sense of “no infarction is missed” in the validation.

1. Introduction

Myocardial ischemia occurs when the blood and oxygen supply to the myocardium is dramatically decreased or interrupted due to, e.g., blockage of a coronary artery. If the condition persists, myocardial infarction will emerge, which leads to a permanent damage to the heart tissue and poses an immediate risk to a patient's life. The objective of the present study is the determination of an optimal electrode configuration of the proposed wearable ECG monitoring system by means of computer simulation. This system is expected to involve a minimal number of electrodes with positions optimized for the detection of acute myocardial infarction. It can be observed, that using only 2 electrodes many infarctions do not show any change in ST-segment and thus cannot be detected (silent infarction). Therefore, utilization of 2 pairs of electrodes is suggested in the current work. Optimum in this work means: no infarction will be missed. For this purpose, an individ-

ual computer model is built from a patient's MRI data-set. The electrical activities in the heart are simulated using a cellular automaton. 153 myocardial infarctions of different sizes and at various sites in the entire left ventricular wall and septum, i.e., 9 infarctions simulated in each AHA segment [1], are simulated and the corresponding body surface potentials are computed using the finite element method. The ST-integral of the body surface electrical potentials of all myocardial infarctions are analyzed by comparing with the simulated healthy body surface potentials (no infarction). According to the analysis, an optimal electrode configuration is obtained, which consists of 4 electrodes. For the validation, 50 additional simulations with infarctions in the left ventricle, whose sites and sizes are randomly generated, are performed. The 50 random infarctions are examined using the suggested optimal electrode configuration and a high sensitivity of 98% is reached.

2. Methods

2.1. Anatomical model

The individual anatomical model of a patient's torso is constructed from MRI-scans with a resolution of $4\text{mm} \times 4\text{mm} \times 4.69\text{mm}$. After segmentation and classification the MRI data-set is converted to a voxel-based model with a resolution of $2\text{mm} \times 2\text{mm} \times 2\text{mm}$. The computer model includes heart, lungs, liver, simplified gastrointestinal tract and other important organs (see Fig. 1a). The heart geometry is built from short axis MRI-scans with a resolution of $2.26\text{mm} \times 2.26\text{mm} \times 4\text{mm}$. The excitation conduction system including bundle branches, fascicles and Purkinje fibers as well as the fiber orientation are built into the ventricular wall (see Fig. 1b). In order to perform the forward and inverse calculations a tetrahedron-based finite element mesh is then generated from the aforementioned voxel-based model. Moreover, the appropriate conductivity values are assigned to different tissue classes in the volume conductor [2–4].

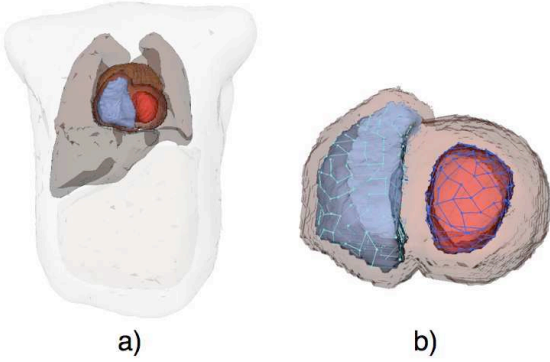


Figure 1. Computer model of a patient: torso (a) and heart (b). The model is shown half transparently.

2.2. Cellular automaton

A rule-based cellular automaton developed at the Institute of Biomedical Engineering, Karlsruhe Institute of Technology, Germany is applied to simulate the excitation propagation in the heart [5]. In the cellular automaton each voxel represents a patch of cardiac cells, which possess the same physiological and electrical properties. A voxel can be activated by the neighboring excited voxels. After activation the state transition of the current element, i.e., change of transmembrane voltage, complies with its action potential curves, which are extracted from the ten Tusscher cardiac cell model [6]. The transmural heterogeneity of myocardium is also taken into account in the modeling. The simulation is conducted in the voxel-based heart model with a spatial resolution of $1mm \times 1mm \times 1mm$ and a time step of $1ms$. The simulation results are saved every $4ms$.

2.3. Modeling of acute myocardial infarction

Normally, myocardial infarction consists of non-excitabile tissue in the center and a border zone presenting the transition from the necrotic tissue to the healthy tissue. In the central region no electrical excitation exists; in the transition zone cardiac cells are still excitable but the activity of the cells is limited. Myocardial infarction can be modeled by changing the local parameters for the excitation amplitude and propagation velocity in the cellular automaton according to the function as illustrated in Fig. 2 [5]. In this modeling a myocardial infarction is defined by 5 parameters, i.e., 3 coordinates of the infarction center, the radius of infarction region in mm and the thickness of the transition zone.

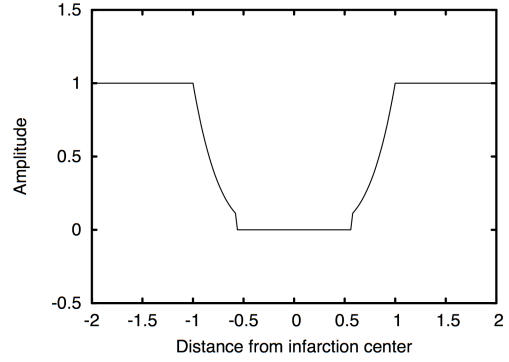


Figure 2. The dependence of excitation amplitude and propagation velocity from the distance to the center of myocardial infarction. The unit length 1 in x-axis indicates the radius of infarction area.

2.4. Forward problem

The forward computation is performed on the finite element mesh. The distribution of the transmembrane voltage at a certain time instant obtained from the cellular automaton is first interpolated from the voxel-based mesh onto the correspondent nodes in the tetrahedron mesh. The potential distribution on the body surface are then calculated by solving the Poisson's equation incorporating the bidomain model [7, 8]

$$\nabla \cdot ((\sigma_i + \sigma_e)\nabla\Phi_e) = -\nabla \cdot (\sigma_i\nabla V_m) \quad (1)$$

applying the finite element method, where σ_i and σ_e are the intracellular and extracellular conductivity tensors; Φ_e and V_m are extracellular potentials and transmembrane voltages, respectively.

2.5. Optimization of electrode positions

In the present study the optimization of electrode positions is based on the analysis of the ST-integral of ECG signal. The ST-integral S_m of one ECG channel, i.e., at one electrode, is defined as the sum of ECG signal at all time instants during the ST-segment. On the torso surface of the patient 663 electrode positions are selected, which are evenly distributed on the model surface. Thus, ST-integrals at these 663 positions are calculated for each myocardial infarction and denoted as S_m with m denoting the index of electrode positions. The ST-integral difference $D_{i,j}$, which can also be interpreted as the ST-integral of the bipolar ECG signal, between every possible combination of 2 electrodes i and j is computed. For each infarction 219122 ST-integral differences are calculated in total. Then every ST-integral difference $D_{i,j}$ is compared with its corresponding reference value $D_{H_{i,j}}$, which comes from the

simulated healthy ECG without infarction. If the difference between $D_{i,j}$ and $D_{H_{i,j}}$ is above or equal to a proper threshold T , this pair of electrodes is able to detect the infarction under the current consideration. If the difference is below the given threshold, this pair of electrodes then fails to detect this infarction. This prescribed procedure will run throughout a comprehensive basis of infarctions, which will be described in detail in the next section. In case that all the infarctions in the basis can be detected by one pair of electrodes, this pair of electrodes will be the optimal electrode configuration for the proposed wearable ECG monitoring system. When only one pair of electrodes is not sufficient to detect all the infarctions, two pairs of electrodes will be utilized. In this case one infarction can be considered as being successfully detected when at least one pair of electrodes can detect the current infarction.

3. Results

3.1. Forward simulation

In the current study the left ventricle including the ventricular septum is subdivided into 17 segments (see Fig. 3b and 3c) according to the recommendation from the American Heart Association (see Fig. 3a) [1,9].

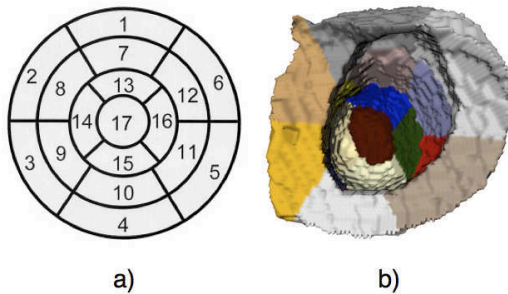


Figure 3. The nomenclature of 17 AHA segments in left ventricle (a) and the subdivision of the left ventricular model according to the AHA suggestion (b).

In each segment 3 types of acute myocardial infarctions are simulated, i.e., subendocardial, transmural and subepicardial infarctions. For each type, 3 different sizes are considered, i.e., $10mm$, $20mm$ and $30mm$ for the radius of infarction area. Thus, 153 different myocardial infarctions are simulated throughout the entire left ventricle and septum, which constructs a comprehensive basis of myocardial infarctions in the left ventricle. As examples, 6 simulated infarctions with various sizes and in different segments are shown in Fig. 4.

By solving the forward problem the corresponding 153 BSPMs are obtained. For the further investigation ST-integrals are calculated. In order to visualize the ST-integrals they are interpolated and shown as ST-integral

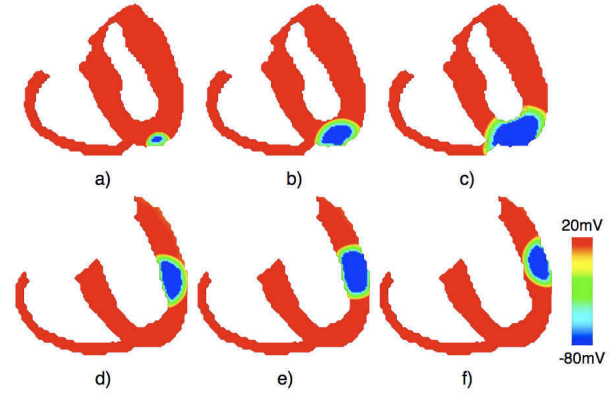


Figure 4. Simulated apex infarctions (segment 17) with radii of $10mm$ (a), $20mm$ (b) and $30mm$ (c); simulated subendocardial (d), transmural (e) and subepicardial (f) infarctions with a radius of $20mm$ in the apical lateral segment (segment 16). The distribution of transmembrane voltages during ST-interval is shown in a cross-section of heart.

maps on the surface of the torso model. 6 ST-integral maps related to the 6 infarctions shown in Fig. 4 are presented in Fig. 5.

3.2. Optimization of electrode positions

According to the investigation no satisfactory result can be obtained with only one pair of electrodes, because the threshold for the difference between $D_{i,j}$ and $D_{H_{i,j}}$ has to be set to a very small value, which will probably lead to difficulties in the measurement. Therefore, 2 pairs of electrodes are selected. In this case the threshold is then set to $0.4mV$, where the first electrode configuration appears, which is able to detect all 153 myocardial infarction in the basis. The optimal electrode configuration with 2 pairs of electrodes is shown in Fig. 5, i.e., one electrode is located on the left chest directly above the heart, one electrode below the fossa jugularis, one electrode on the right chest and one electrode on the left back.

For the validation 50 additional myocardial infarctions are generated. Their sizes are varied from $5mm$ to $35mm$ in radius and their locations are randomly selected in the whole ventricle including the septum. The suggested optimal electrode configuration is able to successfully detect 49 infarctions among 50 random infarctions with the threshold of $0.4mV$.

4. Discussion and conclusions

As can be seen in the last section a high accuracy of 98% is achieved in the validation. The threshold of $0.4mV$ is still in a reasonable level for the routine ECG measurement

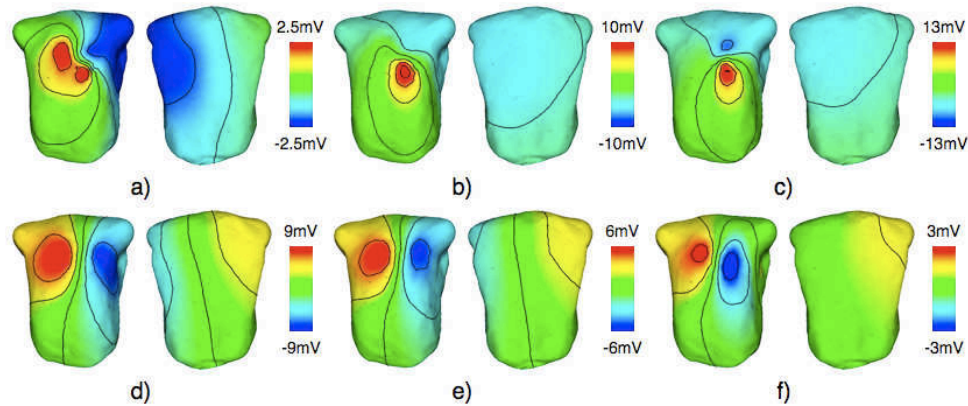


Figure 5. The ST-integral maps corresponding to the simulated apex infarctions (segment 17) with radii of 10mm (a), 20mm (b) and 30mm (c); The ST-integral maps corresponding to the simulated subendocardial (d), transmural (e) and subepicardial (f) infarctions with a radius of 20mm in the apical lateral segment (segment 16).

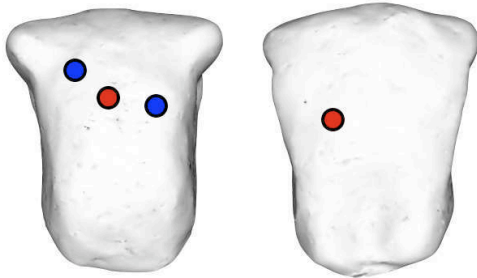


Figure 6. The optimal electrode configuration consisting of 2 pairs of electrodes. One pair of electrodes is shown in red, the other one is in blue.

technique. Moreover, by applying ST-integral the inaccuracy caused by measurement noise can be reduced.

As the next step, more patients will be included in the study to ascertain whether the optimal electrode configuration obtained with the current patient is also applicable for other patients or whether a customized optimal electrode configuration is needed for every individual patient. It is also of interest to investigate the influence of heart motion on the optimization results, because the heart keeps contracting during the entire ST-segment. Hence, a dynamic heart model will be deployed in the further work.

References

- [1] Cerqueira MD, Weissman NJ, Dilsizian V, Jacobs AK, Kaul S, Laskey WK, Pennell DJ, Ryan T, Verani MS. Standardized myocardial segmentation and nomenclature for tomographic imaging of the heart. *Circulation* 2002;105:539–542.
- [2] Gabriel C, Gabriel S, Corthout E. The dielectric properties of biological tissues: I. literature survey. *Physics in Medicine and Biology* 1996;41:2231–2250.

- [3] Gabriel S, Lau R, Gabriel C. The dielectric properties of biological tissues: Ii. measurements in the frequency range 10 hz to 20 ghz. *Physics in Medicine and Biology* 1996; 41:2251–22269.
- [4] Gabriel S, Lau R, Gabriel C. The dielectric properties of biological tissues: Iii. parametric models for the dielectric spectrum of tissues. *Physics in Medicine and Biology* 1996; 41:2271–2293.
- [5] Farina D. Forward and Inverse Problems of Electrocardiography : Clinical Investigations. Ph.D. thesis, Institute of Biomedical Engineering, Universität Karlsruhe (TH), 2008.
- [6] ten Tusscher KHWJ, Noble D, Noble PJ, Panfilov AV. A model for human ventricular tissue. *Am J Physiol Heart Circ Physiol* 2004;Volume 286:1573–1589.
- [7] Miller WT, Geselowitz DB. Simulation studies of the electrocardiogram. i. the normal heart. *Circulation Research* 1978;43(2):301–315.
- [8] Tung L. A Bidomain Model for Describing Ischemic Myocardial D-C Potentials. Ph.D. thesis, M.I.T., Cambridge, Mass., 1978.
- [9] Keller D, Seemann G, Weiss D, Dössel O. Detailed anatomical modeling of human ventricles based on diffusion tensor mri. In *Biomedizinische Technik* 51(1). 2006; .

Address for correspondence:

Yuan Jiang
 Karlsruhe Institute of Technology (KIT)
 Kaiserstrasse 12
 76131 Karlsruhe, Germany
 Yuan.Jiang@kit.edu